scientific reports

Check for updates

OPEN

Reduction of retinal ganglion cell death in mouse models of familial dysautonomia using AAV-mediated gene therapy and splicing modulators

Anastasia Schultz[1], Shun-Yun Cheng[2], Emily Kirchner[3], Stephanann Costello[1], Heini Miettinen[1], Marta Chaverra[1], Colin King[1], Lynn George[1,5], Xin Zhao[6], Jana Narasimhan[6], Marla Weetall[6], Susan Slaugenhaupt[3,4], Elisabetta Morini[3,4], Claudio Punzo[2] & Frances Lefcort[1]✉

Familial dysautonomia (FD) is a rare neurodevelopmental and neurodegenerative disease caused by a splicing mutation in the Elongator Acetyltransferase Complex Subunit 1 (*ELP1*) gene. The reduction in ELP1 mRNA and protein leads to the death of retinal ganglion cells (RGCs) and visual impairment in all FD patients. Currently patient symptoms are managed, but there is no treatment for the disease. We sought to test the hypothesis that restoring levels of Elp1 would thwart the death of RGCs in FD. To this end, we tested the effectiveness of two therapeutic strategies for rescuing RGCs. Here we provide proof-of-concept data that gene replacement therapy and small molecule splicing modifiers effectively reduce the death of RGCs in mouse models for FD and provide pre-clinical foundational data for translation to FD patients.

Familial dysautonomia (FD) is a rare recessive autonomic and sensory neuropathy. Over 99% of FD patients are homozygous for the "founder" mutation in intron 20 of the *ELP1* gene (c.2204 + 6T > C; formerly called "*IKBKAP*"), causing the "skipping" of exon 20 from the mature mRNA coding sequence[1,2]. This mutant mRNA is then targeted for non-sense mediated decay[3]. The mis-splicing occurs in a tissue-specific manner, with peripheral neurons being most impacted, producing almost no functional protein[4,5]. The hallmarks of FD include reduced pain and temperature sensation, gait ataxia, cardiovascular instability, swallowing impairment, gastrointestinal dysfunction, and eventual blindness[6]. As patients age, visual impairment becomes one of the most debilitating symptoms, given that it is accompanied by loss of balance and gait ataxia. The optic neuropathy in FD results from the progressive death of retinal ganglion cells (RGCs) and the loss of their axons from the nerve fiber layer (NFL) in the retina's macular region[7–9].

It is necessary to develop therapeutics to reduce the loss of RGCs that occurs in all FD patients. Being a monogenic disease, FD is a strong candidate for genetic therapies. Gene replacement therapies for retinal diseases show tremendous potential due to the accessibility and immune-privileged status of the eye[10]. Preclinical and clinical studies have demonstrated that adeno-associated viruses (AAVs) are efficient viral vectors for delivering functional genes in hereditary retinal diseases[10–12]. In addition to gene therapy, a potent strategy for treating genetic diseases is using splicing modulator compounds (SMCs) that correct mutations at the messenger RNA level. Such a modifier was recently approved to restore correct splicing in the neurological disorder spinal muscle atrophy[13,14]. SMCs effectively reduce disease phenotypes in FD mouse models[15–17]. However, to date, no gene therapy approaches have been used to introduce wild-type copies of *ELP1* to correct disease phenotypes. Here

[1]Department of Microbiology and Cell Biology, Montana State University, Bozeman, MT, USA. [2]Department of Ophthalmology, Neurobiology and Gene Therapy Center, University of Massachusetts Chan Medical School, Worcester, MA, USA. [3]Center for Genomic Medicine, Massachusetts General Hospital Research Institute, Boston, MA, USA. [4]Department of Neurology, Massachusetts General Hospital Research Institute and Harvard Medical School, Boston, MA, USA. [5]Department of Biological and Physical Science, Montana State University Billings, Billings, MT, USA. [6]PTC Therapeutics, Inc., South Plainfield, NJ 07080, USA. ✉email: lefcort@montana.edu

we present pre-clinical data demonstrating the effectiveness of gene therapy and a novel splicing compound in preventing RGC death in FD mouse models.

Results

Using two complementary FD mouse models, mice were treated either with (1) an intravitreal injection of an AAV2 (highly tropic for RGCs) engineered to express a wild type copy of *ELP1*[18–20] (Fig. 1A) or (2) a novel small molecule splicing modulator to restore correct *ELP1* splicing[16] (Fig. 1B).

To test whether a gene replacement strategy could prevent the death of RGCs in our previously established *Pax6-cre;Elp1*$^{loxp/loxp}$ mouse model[21], we generated two AAV2 vectors, one expressing the murine *Elp1* gene *(mElp1)* and the other expressing *eGFP*, both driven by the U1a promoter (see Methods). We first determined that the AAV2-U1a-*mElp1* could drive the expression of *Elp1* in the mouse retina and increase Elp1 protein expression in vitro (Supplemental Fig. 1; Supplemental Fig. 3A–C).

Next, cohorts of *Pax6cre;Elp1*$^{loxp/loxp}$ mice received intravitreal injections of AAV2-U1a-*mElp1* or control (*eGFP*) vector at postnatal day 21 (P21) before any significant loss of RGCs is observed[21]. Three months following injection, RGCs were quantified by flat-mount analysis (Fig. 2A). This time point was selected since prior work established that, by this age, 40–60% of RGCs have died[21]. We observed a significant response with both the higher AAV2-U1a-*mElp1* vector dose ($\times 10^9$ vg/eye), showing a 137% increase in the average number of RGCs (5696 ± 252 (SEM), $p < 0.0001$) and the lower AAV2-U1a-*mElp1* vector dose ($\times 10^8$ vg/eye), showing a 131% increase in the average number of RGCs (5563 ± 172 (SEM), $p < 0.0001$) in an area of 4mm^2 in *Pax6cre; Elp1*$^{loxp/loxp}$ retinae compared to untreated *Pax6cre; Elp1*$^{floxp/loxp}$ retinae with an average number of 2404 ± 405 (SEM) RGCs 4mm^2 (Fig. 2B). Interestingly, eyes injected with the control AAV2-U1a-*eGFP* showed an 82% increase in the average number of RGCs (4386 ± 534 (SEM)) compared to the untreated *Pax6cre; Elp1*$^{loxp/loxp}$ (Fig. 2B). However, the *mElp1-virus* significantly increased RGC numbers by 30% ($p = 0.04$) above the *eGFP*-injected eyes. This suggests that (1) injection of a virus in a dose-dependent manner alone induces a protective response in the retina, most likely by stimulating a wound response[22–24], but (2) that the *Elp1* virus increased RGCs significantly above

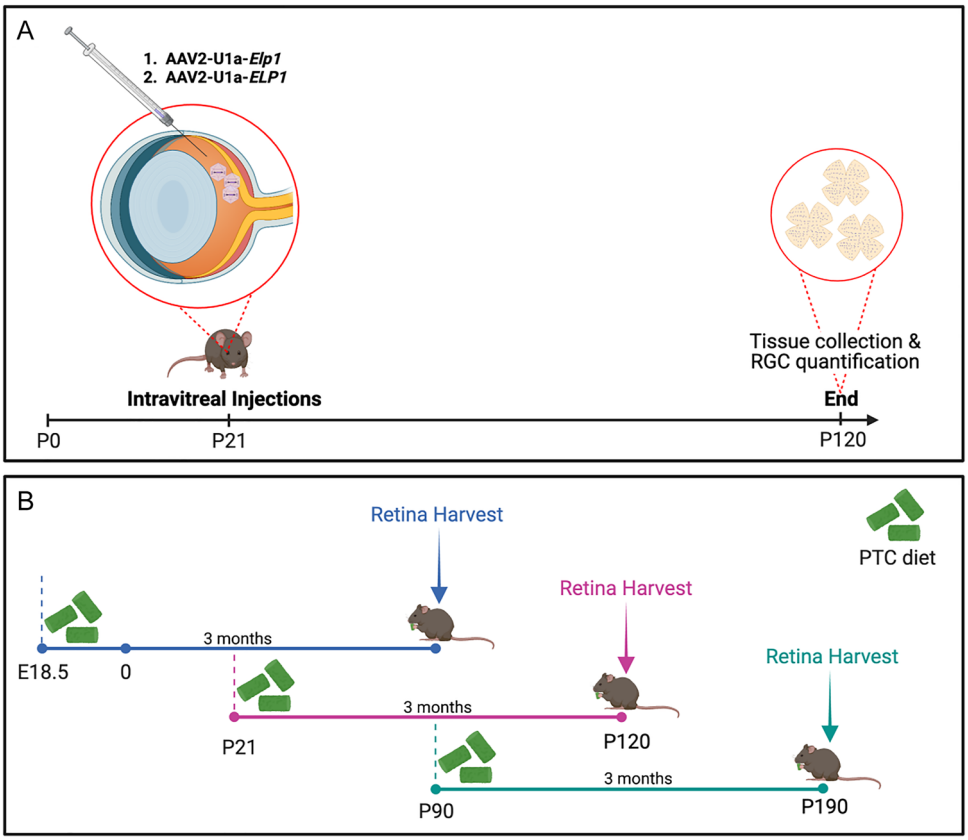

Figure 1. Experimental workflow. (**A**) Mice were intravitreally injected with an AAV2-vector in both eyes at P21, and the retinal ganglion cell (RGC) number was quantified 3 months later. An experimental or control virus was injected into the vitreous humor of the mouse eye, where it can diffuse into the retina and target RGCs. (**B**) FD mutant mice were divided randomly into two groups: control and experimental. The control group was fed a standard chow diet, and the experimental group with a specially formulated chow diet containing a novel splicing modulator compound, PTC680. Groups were started on treatment at three different ages: E18.5, P21 or P90. After 3 months on either the control or experimental diet, retinas were analyzed and quantified for exon 20 inclusion and RGC numbers, respectively. Created with BioRender.com.

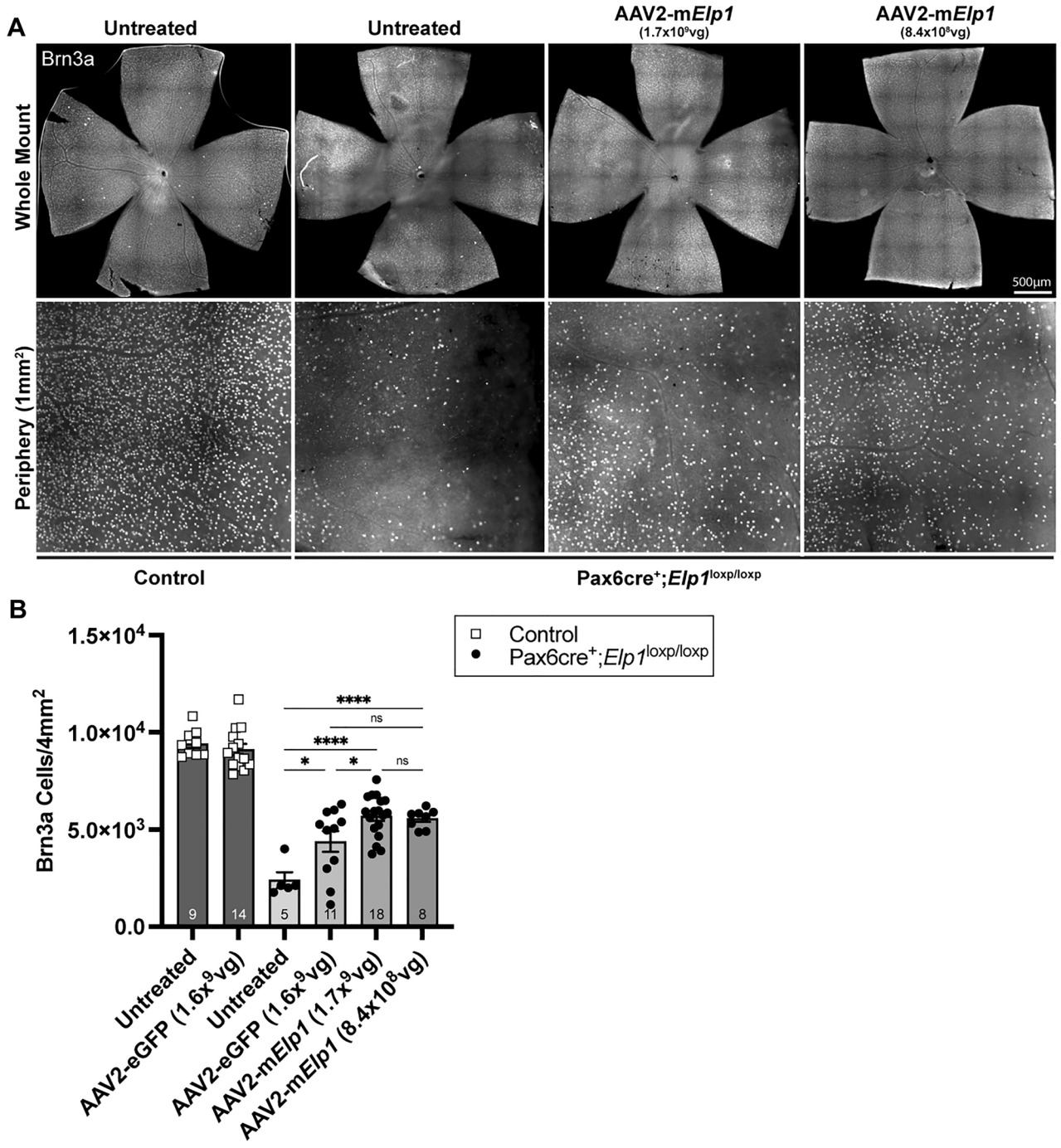

Figure 2. Viral transduction of murine *Elp1* rescues RGCs in a mouse model of FD. (**A**) Representative retinal whole mount (top) and peripheral retina (bottom) 3 months after intravitreal injection with AAV2-U1a-m*Elp1*. RGCs were immunolabeled using an antibody against Brn3a. Scale bar, 500 µm. (**B**) Quantification of Brn3a + RGCs from control mice (dark gray) compared to FD mice (lighter gray gradient) receiving injections at P21 with either the *eGFP* (1.6×10^9 vg/eye) or experimental *mElp1* virus (1.6×10^9 vg/eye, 1.7×10^9 vg/eye, 8.4×10^8 vg/eye). Brn3a + cells were counted in a $1mm^2$ area in each quadrant of the peripheral retina. The adjusted p-values are displayed. ns $p = 0.2, 0.99$, $^*p = 0.02, 0.04$, $^{****}p < 0.0001$, one-way ANOVA with Tukey's multiple comparisons follow-up test. Data are shown as average ± SEM, and each data point represents an individual retina. The sample size for individual groups is represented by *n* within each bar.

the virus-alone-induced protective response. These data provide promising evidence that gene replacement therapy, with further optimization, could be used to ameliorate RGC death in FD.

Based on these data, we generated an AAV2 vector driving the expression of the human *ELP1* gene (*hELP1)*. Again, we confirmed that the AAV2-U1a-*hELP1* could increase ELP1 protein in vitro (Supplemental Fig. 2A,B; Supplemental Fig. 3D) and drive *ELP1 mRNA* expression in wild-type mouse retinas in vivo (Supplemental Fig. 2C). Subsequently, *Pax6cre;Elp1*$^{loxp/loxp}$ and littermate controls were intravitreally injected with three different viral titers of the human *ELP1* virus. All mice received bilateral injections at P21, and RGCs were quantified three months later (Fig. 3A). There was a significant increase in RGC survival in the *Pax6cre;Elp1*$^{loxp/loxp}$ retinae that received the highest vector dose (5.4×10^8 vg/eye), showing a 39% increase in the average number of RGCs (4925 ± 439 (SEM), $p = 0.02$) (Fig. 3B). There was no significant difference between the uninjected retina and those injected with the AAV2-U1a-*eGFP* construct, which was used at a lower dose than in the mouse *Elp1* virus experiments. To visualize the AAV2-U1a-*hELP1* infected RGCs, we double immunolabeled retinae with antibodies to RGCs and human ELP1. In the retinae infected with AAV2-U1a-*hELP1,* approximately 26% of RGCs expressed the human ELP1 protein (Fig. 3C), visually confirming that driving *ELP1* expression can efficiently produce human ELP1 protein.

Another validated approach for treating genetic disease is using orally administered small molecules that modify splicing[25,26]. To test the efficacy of a novel small splicing compound PTC680, an analog to the highly

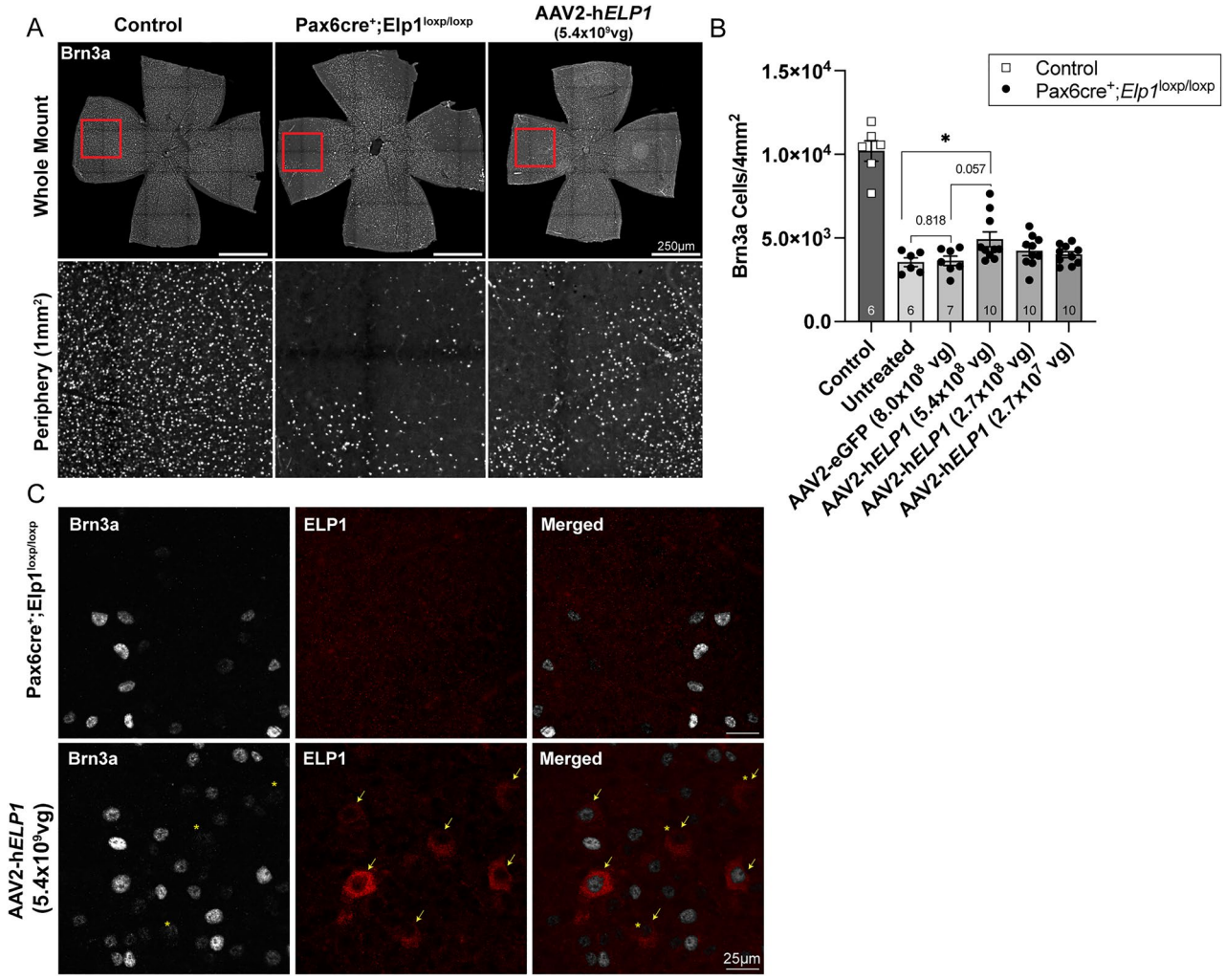

Figure 3. In vivo expression of human *ELP1* prevents loss of RGCs in a mouse model of FD. (**A**) Representative retinal whole mount (top) and peripheral retina (bottom) 3 months after intravitreal injections with *hELP1*. RGCs were immunolabeled using an antibody against Brn3a. Scale bar, 250 µm. (**B**) Quantification of Brn3a + RGCs from control littermate mice (dark gray) compared to FD mice (lighter gray gradient) receiving injections at P21 with either the eGFP (8.0×10^8 vg/eye) or experimental *ELP1* (5.4×10^8 vg/eye, 2.7×10^8 vg/eye, 2.7×10^7 vg/eye) virus. Brn3a + cells were counted in a $1 mm^2$ area in each quadrant of the peripheral retina. (**C**) Representative images of Brn3a + RGCs (gray, yellow asterisks represent lower Brn3a intensities) and the human ELP1 protein expression (red, yellow arrows) 3 months after intravitreal injections into mutant mice. Scale bar, 25 µm. The adjusted p-value is displayed. *$p = 0.02$, ns = 0.818, ns = 0.057; unpaired, two-sided Mann–Whitney U test. There is a statistically significant difference between the untreated FD mice and FD mice receiving the higher dose of AAV2-h*ELP1* 5.4×10^8 vg/eye. Data are shown as average ± SEM, and each data point represents an individual retina. The sample size for individual groups is represented by *n* within each bar.

specific *ELP1* splicing modulator PTC258[16], we generated a new hybrid mouse model in which we introduced the human *FD ELP1* original founder splice mutation (*TgFD9)* transgene into the *Pax6cre;Elp1*$^{loxp/loxp}$ conditional knockout mouse model. This new model recapitulates the FD retinal phenotype while recreating the tissue-specific mis-splicing observed in FD patients. To assess the therapeutic effect of PTC680, we administered an oral treatment formulated to dose each *TgFD9;Pax6cre;Elp1*$^{loxp/loxp}$ mouse 1.2 mg/kg/day. Treatment started at three different time points, (a) Embryonic day 18.5 (E18.5), (b) P21, and (c) P90, to test the therapeutic efficacy throughout the lifespan and disease progression (Fig. 1B). In all cases, mice consumed either vehicle or PTC680 special chow for 3 months. RGCs were quantified at the end of each 3-month treatment regimen using retinal flat-mount analysis (Fig. 4A). PTC680 treatment increased RGC number by up to 57% depending on the age at which treatment began (Fig. 4B). The most significant increase in RGCs occurred when treatment began at the youngest age (E18.5). Notably, a significant rescue of RGCs occurred even when treatment started at 3 months old. Thus, daily consumption of PTC680 prevents significant RGC death in both mature and immature retinas.

To assess whether RGC rescue was associated with increased splicing efficiency of the mutant FD *ELP1* gene, we analyzed *ELP1* splicing in retinal tissue from vehicle- and PTC680-treated FD mice. As demonstrated with PTC258[16], PTC680 significantly increases *ELP1* exon 20 inclusion in the FD retina (Fig. 4C; Supplemental Figs. 4, 5, 6), providing evidence that this novel splicing modulator mitigates a primary FD phenotype by increasing human *ELP1* in the retina.

Discussion

We demonstrate that both an intravitreally-delivered RGC-specific gene transfer and the systemic delivery of a novel small molecule splicing modulator can prevent the progressive death of RGCs in models of FD. This is the first gene therapy study in an FD model and lays the foundation for a translational path for mitigating RGC loss in FD patients. Additionally, we show that in a new mouse model, the oral administration of the novel PTC680 compound significantly improved RGC survival throughout multiple stages of disease progression. These data are encouraging as most FD patients do not report vision loss until they are teenagers.

Our data show that approximately 30% of RGCs were infected with the human *ELP1* virus and expressed the human ELP1 protein, which is in the same range as the percentage of RGCs rescued (39%). Moreover, we provide the first evidence that morphology is not disrupted in RGCs expressing virally transduced *ELP1*, suggesting that overexpression of human *ELP1* is not harmful to retinal neurons. Future studies will be required to test the extent of RGC rescue, i.e., physiological function. One concern is whether the reintroduction of Elp1 protein in RGCs is sufficient to support circuit maintenance with RGC targets in the brain; a second concern, given the broad expression of Elp1 in the brain, is whether visual processing and perception will be improved if RGC inputs are restored.

These data justify the further optimization of an *ELP1*-vector for translation to a clinical setting. Potential paths forward include optimizing the AAV2 capsid properties via chemical modifications or assembling mosaic capsids consisting of different serotypes could improve targeting specificity and tropism to achieve higher transduction efficiency[27–29]. Alternatively, concatamerization of dual AAV vectors[30–34] can be considered as the *ELP1* transgene is large (4 kb), making packaging challenging. This would provide more flexibility in promoter choice to maximize transduction efficiency in RGCs.

FD is a complex developmental and degenerative disease, yet because it is caused by a single splicing-associated point mutation, it is an excellent candidate disease for both gene therapy and small molecule splicing modulators. In summary, the data presented here provide a rationale for translating gene replacement therapy and splicing modulator compounds into the clinic to prevent the progressive optic neuropathy that plagues all FD patients.

Materials and methods

Animals

All mice were housed in the AALAC-accredited Animal Resource Center at Montana State University. All animal use protocols were approved by the Montana State University Institutional Animal Care and Use Committee (IACUC) (protocol No. 2020-15-IA; Bozeman, MT). The study fulfilled the ARRIVE guidelines, and all experiments complied with relevant guidelines and regulations. The generation of the *Pax6cre*$^{+}$*;Elp1*$^{flox/flox}$ CKO is described in Ueki et al., 2018. Briefly, retina-specific *Elp1* CKO mice were generated by crossing Elp1 floxed (International Knockout Mouse Consortium, Wellcome Sanger Institute, UK) and αPax6 promoter-driven Cre (Pax6-Cre) mice[35], which were a gift from Drs Peter Gruss and Ruth Ashery-Padan. This is a useful mouse model to study the FD optic neuropathy due to the restricted deletion of *Elp1* only in retinal neurons with a time course of RGC loss consistent with patients while maintaining a phenotypically healthy mouse.

A new hybrid mouse model, the *TgFD9;Pax6cre;Elp1*$^{loxp/loxp}$ was generated to analyze the splicing compound in a mouse model that expressed the FD founder mutation on a mouse background that was null for mouse *Elp1* in the retina. To this end, we crossed our original *Pax6-cre;Elp1*$^{loxp/loxp}$ mice, with *FD9/FD9; Elp1*$^{loxp/loxp}$ transgenic line that expresses nine copies of the human FD *ELP1* mutation[36]. To ensure that crossing in the *FD9* transgene did not, by itself, rescue the loss of RGCs in the *Pax6cre;Elp1*$^{loxp/loxp}$ model, we quantified RGCs in both models at 3 months and found a ~ 55% reduction, indicating that the low levels of *ELP1* transcribed from the human gene were not sufficient to prevent the death of RGCs.

The sample size for all experiments was based on an A priori power analysis of 90% with an effect size of 2 and α of 0.05 to detect a statistical difference between the experimental and control groups [21; Ueki and Lefcort, unpublished]. Both male and female mice were used at the ages indicated (E18.5 up to 6 months), and all controls were littermate *Pax6cre*$^{-}$*;Elp1*$^{loxp/loxp}$. Mice were randomly assigned to a treatment group based on sex and genotype. All mice were housed in a 12-h light–dark cycle and were fed chow and water ad libitum.

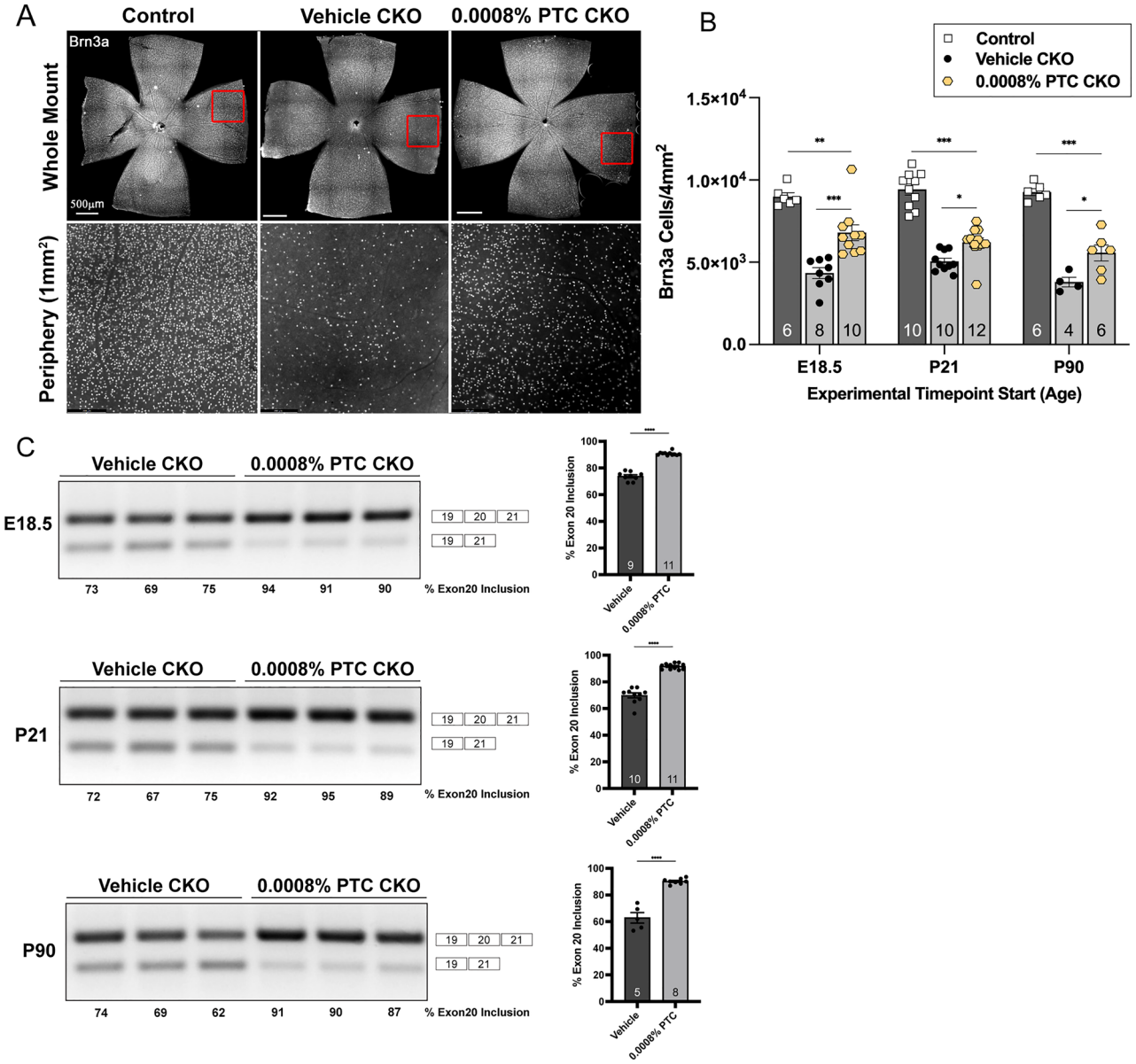

Figure 4. Daily PTC680 consumption protects retinal ganglion cells from cell death and increases full-length *ELP1* transcript in a new retinal FD mouse model. (**A**) Representative retinal whole mount (top) and peripheral retina (bottom) after daily consumption of PTC680 for 3 months. Scale bar, 500 µm. (**B**) Quantification of Brn3a + cells from control littermate mice (dark gray) and FD mice (light gray) on the vehicle or experimental chow. All mice consumed chow for 3 months, but each experiment started when the mice were at a different age: E18.5 (**$p = 0.004$, ***$p < 0.001$), P21 (*$p = 0.01$, ***$p = 0.0000$) or P90 (*$p = 0.02$, *** = 0.0000), to test the efficacy of starting treatment at different time points within disease progression. The adjusted p-values are displayed, one-way ANOVA with Tukey's multiple comparisons follow-up test (**C**) representative splicing analysis of human *ELP1* transcripts and percent of exon 20 inclusion in retinae from vehicle-treated (dark gray) and PTC 0.0008%-treated (light gray) FD mice at the different experimental start times. *This figure only demonstrates exon 20 inclusion in FD mice receiving either the PTC or vehicle treatment alone. All full-length gels can be found in supplemental Figs. 4*, 5 and 6. The adjusted p-values are displayed. ****$p < 0.0001$, two-tailed unpaired Student's *t*-test. Data are shown as average ± SEM, and each data point represents an individual retina. The sample size for individual groups is represented by *n* within each bar. This experiment was conducted three times. Conditional knockout (CKO) = Pax6cre^{+};Elp1$^{loxp/loxp}$.

AAV vector design and production

All AAV viruses were made at the Vector Core in the Gene Therapy Center at the University of Massachusetts Medical School. AAV2 was selected based on its reported tropism for mouse retinal ganglion cells and its use and tolerance in the human eye[37–39] and preliminary experiments by Ueki and Lefcort (unpublished) revealing

its higher expression efficiency in retinal ganglion cells in our mouse line compared to AAV9. The AAV2 was used at vector doses ranging from 8×10^8 to 1.7×10^9 vector genomes per eye (vg/eye) per mouse for the mouse *Elp1*, while the human *ELP1* virus was used at doses ranging from 2.7×10^7 to 5.4×10^8 vg/eye. Vector doses were based on preliminary experiments showing potential viral toxicity at higher doses and evidence for cell rescue at lower doses (data not shown). Each virus expressed the full-length sequence for either mouse *Elp1* (Origene MC202501, NM 026079) or human *ELP1* (Origene RC2076868), ELP1 (NM_003640), and both were driven by a murine small nuclear RNA promoter (U1a). The U1a promoter was selected based on its small size (~ 250 bp) and ability to effectively transduce cells in the central nervous system[40].

Cell culture

Human embryonic kidney cells (HEK293) were gifted from Carolyn Machamer at Johns Hopkins, and the Chinese hamster ovary cell (CHO) cells were gifted from Ira Mellman at Yale University. HEK293 were cultured in Dulbecco's Modified Eagle Medium (DMEM, Gibco #12430-054) supplemented with 10% fetal bovine serum (FBS, Gibco #16000-036), 100 U/ml penicillin/100 µg/ml streptomycin (Corning, #30-002-CI), and 2 mM L-Glutamine (Gibco, #25030-081). HEK293 cells submitted to American Type Culture Collection (ATCC) for STR profiling were an 88% match for the HEK293 cell line, CRL-1573.

In vitro AAV transduction

HEK293 cells were seeded onto a 12-well plate at a density of 2.5×10^4 cells/well for 24 h. Two viral solutions were diluted (1) AAV2-U1a-h*ELP1* stock to 2.7×10^9 VG/ml in DMEM and (2) AAV2-U1a-eGFP stock to 8.8×10^9 VG/ml in DMEM. The *ELP1* solution was serially diluted to three different multiplicities of infection (m.o.i.) at 20 K, 100 K, and 400 K. M.O.I. was calculated by dividing the initial seeding density by the total viral particles. At 24 h, the complete medium was removed and supplemented with the viral medium. Cells proliferated for 6 h in the viral medium. At 30 h, the viral medium was removed and replaced by the complete medium. Cells were harvested 4 days post-transduction (PTD).

Western blot

The western blot analysis was performed as previously described[21]. Briefly, cells were extracted on ice with lysis buffer (25 mM Tris–HCL, pH 7.5, 150 mM NaCl, 1 mM EDTA, 1% NP40, 5% glycerol) containing 1X HALT protease inhibitor cocktail, 1 mM PMSF, and 10 µM Leupeptine. A Bradford 1X protein–dye reagent (Bio-Rad #5000205) was used to determine the protein concentration. 25 µg of protein was separated by electrophoresis in an SDS–polyacrylamide gel, and the proteins were transferred onto a PVDF membrane. The membrane was blocked for 1 h in 5% non-fat dry milk (NFDM) in 1X Tris-buffered saline containing 0.1% Tween-20. The membrane was incubated with primary antibodies overnight at 4 °C. The primary antibodies to rabbit anti-Elp1 (1:1500) (Anaspec, #AS_54494)) and rabbit anti-GFP (1:2000) (Invitrogen, RRID: AB_221569) were diluted in 1X TBS containing 5% BSA and 0.1% Tween-20. Following primary incubation, membranes were probed with a secondary antibody (Horseradish peroxidase-conjugated goat anti-rabbit IgG (Jackson Laboratories, #111–035-144), 1:10,000 dilution, in 1X TBS containing 5% NFDM and 0.1% Tween-20. Quantitative analysis was performed using Image J (NIH, USA) software, and bands were normalized to total protein and the housekeeping gene *Gapdh* (1:10,000, Millipore, NP_002037).).

RT-qPCR

Real-time PCR (RT-qPCR) was used to quantify mRNA collected from snap-frozen retinal tissue. Total RNA was isolated and purified using the Direct-zol RNA mini-prep kit (Zymo Research, #R2050). The RNA concentration and purity was measured using BioTek Epoch 2 microplate spectrophotometer. 25 ng of purified RNA was reverse transcribed using SuperScript IV VILO mastermix (Invitrogen, #11756050). qPCR was performed with cDNA equivalent of 25 ng of transcribed RNA using SYBR Green master mix (Bio-Rad, #336501) using the 7500 Fast Real-Time PCR system (Fisher Scientific, Applied Biosystems, #4351106). The cycling condition was performed per the manufacturer's protocol (Bio-Rad). All primers (Supplemental file 1) were designed using NIH Primer-Blast tool. The relative expression analysis was performed using the delta delta CT method (ΔΔCT) and expressed as fold change normalized to the average of the two housekeeping genes.

RT-PCR analysis of *ELP1* transcripts

Retinae were snap-frozen in a dry-ice bath with 95% EtOH upon collection. Tissues were homogenized in ice-cold TRI reagent (Molecular Research Center, Inc., Cincinnati, OH, USA), using a TissueLyser (Qiagen). Total RNA was extracted using the TRI reagent procedure provided by the manufacturer. RNA quality and yield was determined using a Nanodrop ND-1000 spectrophotometer. Reverse transcription was performed with 500 ng of total RNA, random primers, and Superscript™III reverse transcriptase (Invitrogen). PCR was performed for the splicing analysis with the 3 µl of cDNA in a total volume of 20 µl with GoTaq Polymerase 2X (Promega) and 32 amplification cycles. We used human-specific *ELP1* primers—forward, 5′-CCTGAGCAG CAATCATGTG-3′; reverse, 5′-TACATGG TCTTCGTGACATC-3′ to amplify human *ELP1* expressed from the transgene. The PCR products were separated on 1.5% agarose gels for 2.5 h at 90 V. The relative amounts of WT and mutant (Δ20) *ELP1* spliced isoforms in a single PCR were determined using ImageJ and the integrated density value for each band as previously described[41,42]. The relative proportion of the WT isoform detected in a sample was calculated as a percentage.

Intravitreal injections

Three-week-old mice were anesthetized by isoflurane inhalation. Prior to anesthesia the pupil was dilated with one drop of phenylephrine (Phenylepherine Hydrochloride Ophthalmic Solution, USP 10%; National Drug Code, [NDC] 42702-103-05, Paragon, BioTeck, Inc) and one drop of tropicamide (Tropicamide Ophthalmic Solution, USP 1%, [NDC] 17478-102-12, Akorn Pharmaceuticals).

Two different intravitreal injection techniques (Manual Hamilton Syringe and WPI-UMP3 with Mirco2T Injector) were used to determine the optimal system for viral delivery. Each eye was treated as an independent experimental endpoint. All control-treated eyes were injected with an AAV2 preparation expressing *eGFP* at 1.6×10^9 or 8.0×10^8 viral genomes. Experimental-treated eyes were tested in a dose-dependent manner to optimize transduction efficiency and RGC rescue. Experimental-treated eyes receiving the AAV2-U1a-*Elp1* were injected with 1.6×10^9, 1.77×10^9, 8.3×10^8, or 8.6×10^8 viral genomes of murine *Elp1*. Experimental-treated eyes receiving the AAV2-U1a-*ELP1* were injected with either 5.4×10^8, 2.7×10^8, or 2.7×10^7 vector genomes of human *ELP1*.

Manual Hamilton syringe

Using forceps, the eyelids were pushed back to expose the cornea. With a 32-G, a small hole was made at the margin of the cornea and sclera. This was necessary because the A 34-G needle (#W1690678) had a blunt tip. The 5 µl calibrated Hamilton #65 needle was inserted at the margin of the sclera and cornea and into the vitreous cavity and 1 µl of the viral solution was injected slowly into the cavity. The needle was left in position for another 15 s and removed slowly.

WPI-UMP3 with Mirco2T Injector (#0916C)

Using forceps, the eyelids were pushed back to expose the cornea. A 36-G beveled needle (NF36BV) attached to a 10 µl Hamilton NANOFIL syringe (WPI, lot# 08C) was inserted at the margin of the sclera and cornea and into the vitreous cavity. Each eye was injected with 600 nL of AAV preparation bilaterally with a 200 nL/sec delivery rate. The needle was left in position for another 10 s to allow the pressure in the injection system to equilibrate with the pressure in the eye and removed slowly. After all surgeries, Puralube® Vet Ointment (Dechra Veterinary Products) was placed on the eye per IACUC guidelines. Mice were monitored and kept on a 37 °C heating pad until awake and recovered and then transferred to their home cage and monitored for 1 to 2 h. Mice remained in their home cage with cage mates until analysis, 3 months after treatment.

Oral administration of splicing compound using a formulated diet

The newly hybrid transgenic mice carrying the human *ELP1* transgene with FD mutation *TgFD9;Pax6cre;Elp1*$^{flox/flox}$ were fed a special diet containing 0.0008% of PTC-409680 (Purina Prolab 3000 with PTC-409680, #21032505A2i) corresponding to a daily consumption of 1.2 mg/kg/day.

Retinal histology following ocular gene therapy with AAV2-U1a-m*Elp1*

Retina flat mount dissection and histology were performed as previously described[43,44]. In brief, Mice were euthanized with CO_2 and the temporal surface of the eye was marked with a green tattoo dye (Ketchum Manufacturing) prior to enucleation. After the eyes were enucleated, a hole was made at the sclera-cornea margin and fixed overnight at 4 °C in 4% PFA. Before antibody staining, the neural retinal layer was detached from the retinal pigment epithelium (RPE)/choroid layer. Rabbit anti-Brn3a (1:300; Synaptic Systems, Cat#411 003) was used as the primary antibody. Brn3 was chosen for quantification because it is a well-established nuclear marker of RGCs, and while it only labels ~ 80% of RGCs, it allowed for more consistent and reliable quantification than the antibody to the RNA-binding protein with multiple splicing (RBPMS), which is expressed in the cytoplasm. Cy3 conjugated anti-rabbit (1:500, donkey) secondary antibody was purchased from Jackson Immuno Research. All antibodies were diluted in 1X PBS with 0.3% Triton X-100 and 5% bovine serum albumin (BSA, Cell Signaling Technology).

Retinal histology following ocular gene therapy with AAV2-U1a-h*ELP1*

Mice were euthanized as stated above. Eyes were fixed at room temperature (RT) for 1 h in 4% PFA. Retinae were then removed, with the temporal region marked by a small cut, and incubated in 4% PFA for an additional 15 min at RT. Tissue was permeabilized in 1X PBS containing 0.5% Triton X-100 for 30 min at RT. Non-specific binding was blocked by incubation with 5% BSA containing 0.5% Triton X-100 for 3 h at RT. All retinae were incubated for 2 nights at 4 °C in a primary antibody solution containing 2% BSA, 0.2% Triton X-100, an anti-Brn3 antibody (1:200, Santa Cruz, #sc-6026), and an anti-ELP1(IKAP) antibody (2 µm/ml, Invitrogen, #PA5-111296, RRID AB_2856706). After overnight incubation at 4 °C with secondary antibodies (Donkey anti-Goat IgG (H + L) Cross-Adsorbed Secondary Antibody, Alexa Fluor™ 647 and Donkey anti-Rabbit IgG (H + L) Highly Cross-Adsorbed Secondary Antibody, Alexa Fluor™ 568 from Thermo Fisher Scientific, catalog # A-21447, RRID AB_2535864 and catalog # A10042, RRID AB_2534017), four identical cuts were made to flatten the tissue into four lobes, and the tissue was mounted with Prolong Gold (Invitrogen).

RGC quantification

Flat mounts were imaged and tiled using a Leica DM6 Thunder microscope at a 10X magnification. For the AAV2-h*ELP1* injected retinae, flat mount images were obtained with a Leica DMi8 THUNDER imaging system using the navigator spiral scan at a 10X magnification. IMARIS software (Oxford Instruments) was used to quantify the number of Brn3a + cells. To identify Brn3a + cells, the spots module was used. The detected diameter

was set at 8 μm in the peripheral region determined by a 1 mm^2 box placed at the edge of each quadrant in regions with the most cell death. If a specific region was damaged, the RGCs directly adjacent were counted. If any complication with the intravitreal injection, retinal harvest, or histology resulted in overall damaged retinal tissue, the sample was excluded and omitted from the analysis. The experimenters were blind to genotype and treatment group for all RGC quantification. The total peripheral cell count is the sum of the cells counted in the four peripheral regions. We analyzed and counted all the Brn3a + RGCs across the entire retina but only report data from the peripheral retina because the *Pax6-Cre* is not expressed in the central retina. Therefore, the loss of Elp1 is restricted only to the periphery[21].

Statistics

All data are expressed as mean ± SEM. Column data are plotted as a scattered dot-bar plot to show variability, and n shows the sample size for each data set. GraphPad Prism (version 9) was used to make all graphs. $p < 0.05$ was considered to represent a significant difference. Following confirmation of normal distribution, data were analyzed using an unpaired two-tailed student's t-test and/or one-way ANOVA followed by Tukey's post hoc test for multiple comparisons.

For AAV2-h*ELP1* injection data, we visually checked normality, found a non-normal distribution, and confirmed with a Shapiro test ($p = 7.89e^{-8}$). Due to non-normal distribution, we ran a Kruskal Wallis non-parametric test ($p = 0.0005$). Followed by a post hoc Dunn test with Bonferroni correction, we found significance only between controls and *Pax6cre;Elp1*$^{loxp/loxp}$ mice, regardless of treatment. Since we had a small sample size with unequal variance and were most interested in the relationship between the uninjected *Pax6cre;Elp1*$^{loxp/loxp}$ and the *Pax6cre;Elp1*$^{loxp/loxp}$ receiving the higher dose of 5.4×10^8 vg/eye, we tested for normality and found a non-normal distribution. Therefore, using a Mann–Whitney U test, we reject the null hypothesis that the distributions are equal and conclude there is a difference between uninjected *Pax6cre;Elp1*$^{loxp/loxp}$ and the *Pax6cre;Elp1*$^{loxp/loxp}$ that received the highest vector dose ($p = 0.02$). All statistics were performed using GraphPad Prism (version 9) and R version 4.2.1 (R Core Team, 2022).

Data availability

All data needed to assess the conclusions from the study are included in the paper and/or supplemental files. When applicable, individual data points are shown on each graph. Please address any requests for raw data counts to the corresponding author.

Materials availability

The newly designed AAV2 vectors are publicly available from Vector Core in the University of Massachusetts Medical School Gene Therapy Center.

Received: 20 May 2023; Accepted: 18 October 2023
Published online: 30 October 2023

References

1. Anderson, S. L. *et al.* Familial dysautonomia is caused by mutations of the IKAP gene. *Am. J. Hum. Genet.* **68**(3), 753–758 (2001).
2. Slaugenhaupt, S. A. *et al.* Tissue-specific expression of a splicing mutation in the IKBKAP gene causes familial dysautonomia. *Am. J. Hum. Genet.* **68**(3), 598–605 (2001).
3. Boone, N. *et al.* Olfactory stem cells, a new cellular model for studying molecular mechanisms underlying familial dysautonomia. *PLoS ONE* **5**(12), e15590 (2010).
4. Cuajungco, M. P. *et al.* Hereditary dysautonomias: Current knowledge and collaborations for the future. *Clin. Auton. Res.* **13**(3), 180–195 (2003).
5. Dietrich, P. & Dragatsis, I. Familial dysautonomia: Mechanisms and models. *Genet. Mol. Biol.* **39**(4), 497–514 (2016).
6. Norcliffe-Kaufmann, L., Slaugenhaupt, S. A. & Kaufmann, H. Familial dysautonomia: History, genotype, phenotype and translational research. *Progress Neurobiol.* **152**, 131–148 (2017).
7. Kfir, J. *et al.* Longitudinal changes in the macula and optic nerve in familial dysautonomia. *J. Neurol.* **268**(4), 1402–1409 (2021).
8. Mendoza-Santiesteban, C. E. *et al.* Selective retinal ganglion cell loss in familial dysautonomia. *J. Neurol.* **261**(4), 702–709 (2014).
9. Mendoza-Santiesteban, C. E. *et al.* Pathological confirmation of optic neuropathy in familial dysautonomia. *J. Neuropathol. Exp. Neurol.* **76**(3), 238–244 (2017).
10. Dhurandhar, D. *et al.* Gene therapy in retinal diseases: A review. *Indian J. Ophthalmol.* **69**(9), 2257–2265 (2021).
11. Bennett, J., & Maguire, A.M. Lessons learned from the development of the first FDA-approved gene therapy drug, Voretigene Neparvovec-rzyl. *Cold Spring Harb. Perspect. Med.* (2022).
12. Li, C. & Samulski, R. J. Engineering adeno-associated virus vectors for gene therapy. *Nat. Rev. Genet.* **21**(4), 255–272 (2020).
13. Baranello, G. *et al.* Risdiplam in type 1 spinal muscular atrophy. *N. Engl. J. Med.* **384**(10), 915–923 (2021).
14. Mercuri, E. *et al.* Safety and efficacy of once-daily risdiplam in type 2 and non-ambulant type 3 spinal muscular atrophy (SUNFISH part 2): A phase 3, double-blind, randomised, placebo-controlled trial. *Lancet Neurol.* **21**(1), 42–52 (2022).
15. Chekuri, A. *et al.* Selective retinal ganglion cell loss and optic neuropathy in a humanized mouse model of familial dysautonomia. *Hum. Mol. Genet.* **31**(11), 1776–1787 (2022).
16. Morini, E. *et al.* Development of an oral treatment that rescues gait ataxia and retinal degeneration in a phenotypic mouse model of familial dysautonomia. *Am. J. Hum. Genet.* **110**(3), 531–547 (2023).
17. Morini, E. *et al.* ELP1 splicing correction reverses proprioceptive sensory loss in familial dysautonomia. *Am. J. Hum. Genet.* **104**(4), 638–650 (2019).
18. Cao, X. *et al.* Factors governing the transduction efficiency of adeno-associated virus in the retinal ganglion cells following intravitreal injection. *Gene Ther.* **26**(3–4), 109–120 (2019).
19. Nieuwenhuis, B., et al., Improving adeno-associated viral (AAV) vector-mediated transgene expression in retinal ganglion cells: comparison of five promoters. *Gene Ther.* (2023).
20. Wassmer, S. J. *et al.* XIAP protects retinal ganglion cells in the mutant ND4 mouse model of leber hereditary optic neuropathy. *Investig. Ophthalmol. Vis. Sci.* **61**(8), 49 (2020).

21. Ueki, Y., Shchepetkina, V. & Lefcort, F. Retina-specific loss of Ikbkap/Elp1 causes mitochondrial dysfunction that leads to selective retinal ganglion cell degeneration in a mouse model of familial dysautonomia. *Dis. Model Mech.* **11**(7), dmm033746 (2018).
22. Steinberg, R. H. Survival factors in retinal degenerations. *Curr. Opin. Neurobiol.* **4**(4), 515–524 (1994).
23. Lau, D. *et al.* Retinal degeneration is slowed in transgenic rats by AAV-mediated delivery of FGF-2. *Investig. Ophthalmol. Vis. Sci.* **41**(11), 3622–3633 (2000).
24. Cao, W. *et al.* Mechanical injury increases bFGF and CNTF mRNA expression in the mouse retina. *Exp. Eye Res.* **65**(2), 241–248 (1997).
25. Oskoui, M., et al., Two-year efficacy and safety of risdiplam in patients with type 2 or non-ambulant type 3 spinal muscular atrophy (SMA). *J. Neurol.* 1–16 (2023).
26. Paik, J. Risdiplam: A review in spinal muscular atrophy. *CNS Drugs* **36**(4), 401–410 (2022).
27. Byrne, L. C., et al., In vivo-directed evolution of adeno-associated virus in the primate retina. *JCI Insight* **5**(10) (2020).
28. Frederick, A. *et al.* Engineered capsids for efficient gene delivery to the retina and cornea. *Hum. Gene Ther.* **31**(13–14), 756–774 (2020).
29. Öztürk, B. E. *et al.* scAAVengr, a transcriptome-based pipeline for quantitative ranking of engineered AAVs with single-cell resolution. *Elife* **10**, e64175 (2021).
30. Carvalho, L. S. *et al.* Evaluating efficiencies of dual AAV approaches for retinal targeting. *Front. Neurosci.* **11**, 503 (2017).
31. Dyka, F. M. *et al.* Dual ABCA4-AAV vector treatment reduces pathogenic retinal A2E accumulation in a mouse model of autosomal recessive stargardt disease. *Hum. Gene Ther.* **30**(11), 1361–1370 (2019).
32. Maddalena, A. *et al.* Triple vectors expand AAV transfer capacity in the retina. *Mol. Ther.* **26**(2), 524–541 (2018).
33. McClements, M. E. *et al.* An AAV dual vector strategy ameliorates the Stargardt phenotype in adult Abca4(−/−) mice. *Hum. Gene Ther.* **30**(5), 590–600 (2019).
34. Trapani, I. Dual AAV vectors for Stargardt disease. *Methods Mol. Biol.* **1715**, 153–175 (2018).
35. Marquardt, T. *et al.* Pax6 is required for the multipotent state of retinal progenitor cells. *Cell* **105**(1), 43–55 (2001).
36. Morini, E. *et al.* Sensory and autonomic deficits in a new humanized mouse model of familial dysautonomia. *Hum. Mol. Genet.* **25**(6), 1116–1128 (2016).
37. Bennett, J. *et al.* Safety and durability of effect of contralateral-eye administration of AAV2 gene therapy in patients with childhood-onset blindness caused by RPE65 mutations: A follow-on phase 1 trial. *The Lancet* **388**(10045), 661–672 (2016).
38. Koilkonda, R. *et al.* LHON gene therapy vector prevents visual loss and optic neuropathy induced by G11778A mutant mitochondrial DNA: Biodistribution and toxicology profile. *Investig. Ophthalmol. Vis. Sci.* **55**(12), 7739–7753 (2014).
39. Harvey, A. R. *et al.* Intravitreal injection of adeno-associated viral vectors results in the transduction of different types of retinal neurons in neonatal and adult rats: A comparison with lentiviral vectors. *Mol. Cell Neurosci.* **21**(1), 141–157 (2002).
40. Buck, T. M. & Wijnholds, J. Recombinant adeno-associated viral vectors (rAAV)-vector elements in ocular gene therapy clinical trials and transgene expression and bioactivity assays. *Int. J. Mol. Sci.* **21**(12), 4197 (2020).
41. Hims, M. M. *et al.* A humanized IKBKAP transgenic mouse models a tissue-specific human splicing defect. *Genomics* **90**(3), 389–396 (2007).
42. Shetty, R. S. *et al.* Specific correction of a splice defect in brain by nutritional supplementation. *Hum. Mol. Genet.* **20**(21), 4093–4101 (2011).
43. Cheng, S.-Y. *et al.* Altered photoreceptor metabolism in mouse causes late stage age-related macular degeneration-like pathologies. *Proc. Natl. Acad. Sci.* **117**(23), 13094–13104 (2020).
44. Cheng, S. Y. *et al.* Low-dose recombinant adeno-associated virus-mediated inhibition of vascular endothelial growth factor can treat neovascular pathologies without inducing retinal vasculitis. *Hum. Gene Ther.* **32**(13–14), 649–666 (2021).

Acknowledgements

We thank Dr. James Fox in the Animal Resource Center at Montana State University for his support and help with animal husbandry. We also thank Jamie Morgan and Luke Domanico at Montana State University for assisting with the cell culture and viral transduction experiments and Dr. Marc Mergy for surgical assistance.

Author contributions

F.L., C.P., E.M., and S.S. supervised and oversaw the experimental approach and conceptualization. A.S., F.L., C.P. and E.M. designed this study. A.S., S.C., C.K., and H.M. conducted experiments. A.S., S.-Y.C., E.K., H.M., and M.C. collected the data. A.S. and S.-Y.C. performed data analysis. X.Z., J.N., and M.W. designed and contributed the chow containing the small splicing modulator. L.G. supervised animal husbandry and breeding strategies. A.S. and F.L. drafted the manuscript. A.S., S.-Y.C., E.K., H.M., M.C., L.G., S.C., C.P., F.L., and E.M. edited the manuscript. All authors read and approved the final manuscript.

Funding

This work was supported by NIH NEI R21EY031130 and a Clare and Phillip Wexler Research Fund grant from the Familial Dysautonomia Foundation.

Competing interests

The authors declare competing financial interests. Xin Zhao, Jana Narasimhan, and Marla Weetall are employees of PTC Therapeutics, Inc., a biotechnology company. In connection with such employment, the authors receive salary, benefits, and stock-based compensation, including stock options, restricted stock, other stock-related grants, and the right to purchase discounted stock through PTC's employee stock purchase plan. Susan A. Slaugenhaupt is a paid consultant to PTC Therapeutics and is an inventor on several U.S. and foreign patents and patent applications assigned to the Massachusetts General Hospital, including U.S Patents 8,729,025 and 9,265,766, both entitled "Methods for altering mRNA splicing and treating familial dysautonomia by administering benzyladenine," filed on August 31, 2012 and May 19, 2014 and related to use of kinetin; and U.S. Patent 10,675,475 entitled, "Compounds for improving mRNA splicing" filed on July 14, 2017 and related to use of BPN-15477. Elisabetta Morini and Susan A. Slaugenhaupt are inventors on an International Patent Application Number PCT/US2021/012103, assigned to Massachusetts General Hospital and PTC Therapeutics entitled "RNA Splicing Modulation" related to use of BPN-15477 in modulating splicing. No other authors declare any competing interests.

Additional information

Supplementary Information The online version contains supplementary material available at https://doi.org/10.1038/s41598-023-45376-w.

Correspondence and requests for materials should be addressed to F.L.

Reprints and permissions information is available at www.nature.com/reprints.

Publisher's note Springer Nature remains neutral with regard to jurisdictional claims in published maps and institutional affiliations.